Morphology and Mechanical Properties of Polypropylene/Polyamide 6 Nanocomposites Prepared by a Two-Step Melt-Compounding Process

Markus Gahleitner,[1] Bernd Kretzschmar,[2] Doris Pospiech,[2] Elisabeth Ingolic,[3] Norbert Reichelt,[1] Klaus Bernreitner[1]

[1]*Polyolefin R&D, Borealis GmbH, St. Peterstraße 25, A-4021 Linz, Austria*
[2]*Institute of Polymer Research Dresden, Hohe Straße 6, D-01069 Dresden, Germany*
[3]*Center for Electron Microscopy Graz, Steyrergasse 17, A-8010 Graz, Austria*

Received 19 November 2004; accepted 15 June 2005
DOI 10.1002/app.23102
Published online in Wiley InterScience (www.interscience.wiley.com).

ABSTRACT: Polypropylene/polyamide 6 blends and their nanocomposites with layered silicates or talc were prepared in a melt-compounding process to explore their mechanical performance. The thermomechanical behavior, crystallization effects, rheology, and morphology of these materials were studied with a wide range of experimental techniques. In all cases, the inorganic filler was enriched in the polyamide phase and resulted in a phase coarsening of the polypropylene/polyamide nanocomposite in comparison with the nonfilled polypropylene/polyamide blend. The mechanical properties of these nanoblends were consequently only slightly better than those of the pure polymers with respect to the modulus, whereas the impact level was below that of the pure polymers, reflecting the heterogeneity of the nanoblend. Polymer-specific organic modification of the nanoclays did not result in a better phase distribution, which would be required for better overall performance.
 J Appl Polym Sci 100: 283–291, 2006

Key words: blends; clay; mechanical properties; morphology; nanocomposites; rheology

INTRODUCTION

Especially for demanding technical applications, for which a high constructional load should be sustained, polypropylene (PP) and its compounds suffer from shortcomings in the elastic modulus and maximum usage temperature. Also, a combination of both (i.e., a reduction of the modulus with increasing temperature) is considered critical even for advanced compounds based on PP. With a steady increase in the crystallinity of PP in combination with the application of special mineral fillers, the limits have been shifted in recent years, but the frontline of mechanical performance can only be reached with long glass fibers, which severely limit the processability and surface appearance.[1–4]

Polyamide 6 (PA-6), especially when combined with fillers, can reach higher stiffness and heat deflection temperature levels. The problems associated with this material are more connected to the water absorption, which not only reduces the mechanical strength but also results in degradation by hydrolysis. This behavior becomes even worse in contact with more aggressive chemicals.

The combination of the mechanical properties and chemical resistance of PA-6 and PP by mechanical mixing (blending) has been tried before in reactive and nonreactive blends of these two polymers. One of the key problems in balancing the properties of such systems is the necessity of using a compatibilizer to achieve a reasonable impact strength through an increase in the phase adhesion between the blend phases. The compatibilizers usually applied, however, limit the modulus level.[5–9] The combination of such systems with mineral fillers has mostly had limited success so far; only glass fibers appear to be interesting,[10,11] but they have the aforementioned negative side effects.

In the study presented here, the possibility of combining PA-6 reinforced with nanoparticles, mainly organophilic montmorillonite, with PP to create blends with superior mechanical performance was investigated. The very small and highly anisotropic particles resulting from the exfoliation of clay have demonstrated a strong reinforcing potential in polycondensates such as PA-6,[12–16] while not damaging processability and surface appearance. When applied to the reinforcement of polyolefins, the problems of disper-

Correspondence to: M. Gahleitner (markus.gahleitner@borealisgroup.com).
Contract grant sponsor: Austrian Forschungsförderungsfonds für die Gewerbliche Wirtschaft; contract grant number: 805.210.

sion and exfoliation are much greater because of the large difference in the polarity between the polymer matrix and clay. A combination in the form of a polar/apolar thermoplastic blend appeared, therefore, to be of interest.

BACKGROUND AND EARLIER WORK

The area of PP/PA-6 blends was investigated intensely in both academia and industrial research, especially in the early 1990s. A large number of publications have been published in the field,[17–20] and the composition effects of these materials, as well as the morphology, rheology, and mechanical performance range, are rather well understood. The use of a compatibilizer—whether added as a separate component or created in situ through reactive modification—is indispensable for achieving a finely disperse phase structure and acceptable mechanics.

Studies on the reinforcement of such blends with mineral fillers and glass fibers have been published to a lesser extent,[10,11] although it is well known that these materials have been investigated, especially in industrial research. This fact is well documented by a number of patents.[21,22]

Nanocomposites based on thermoplastic polymers and clay minerals, specifically with organically modified montmorillonite or similar clay minerals, are a group of materials that have been investigated with growing intensity since the beginning of the 1990s. An extensive review of such hybrid materials has been published recently,[23] summarizing the academic and industrial aspects of their preparation, characterization, and properties.

Among these materials, combinations of PA-6 and organophilic montmorillonite are, again, a well-documented class of thermoplastic engineering materials with high performance. Various aspects, such as the matrix molecular weight effects,[12] mixing energy influence,[13] crystallization,[14,15] and processing behavior,[16] have been studied in detail. Although the market penetration of these materials has so far been less fast than originally predicted, the patent coverage is already rather high.[24,25] Two possible methods of production have been studied: the in situ polymerization of ε-caprolactam after the impregnation of the clay and the melt compounding of the polymer and nanofiller.

The use of nanofillers in PP/PA-6 blends has so far not been investigated thoroughly. Just four examples of such kinds of combination have been found in the literature:

- Liu et al.[26] attempted to reduce the inherent brittleness of a PA-6 nanocomposite by adding maleic anhydride (MAH) grafted PP (PP-*g*-MAH).
- Tjong et al.[27] used a PP–vermiculite nanocomposite as reinforcing phase for PA-6 (although the actual morphology and state of exfoliation of the final composition were not fully clear in this case).
- Chow et al.[28] prepared one-step compounds of PP, PA-6, PP-*g*-MAH, and an organophilic nanoclay by melt mixing (this study already demonstrated two important facts: the nanoclay concentration was much higher in the PA-6 phase, and the modulus increase of the combined system achievable with 4 wt % nanoclay was significantly less than that for pure PA-6 (23 vs 60%)].
- Tang et al.[29] experimented with various mixing sequences of PP, PA-6, PP-*g*-MAH, and an organophilic nanoclay at constant compositions, finding the order of addition to affect the final structure (apart from the predominance of a nanoclay presence in the PA-6 phase, some cases of a labyrinth structure, in which the clay was found mainly at the interface between the two polymers, were described).

EXPERIMENTAL

Materials and compounding

A high-molecular-weight PP homopolymer, BE50 (Borealis, Schwechat, Austria), was used as one of the

TABLE I
Investigated Compositions

No.	PA-6 (wt %)	PP (wt %)	SEBS-g-MAH (wt %)	PP-g-MAH (wt %)	Filler 1		Filler 2		MFR (g/10 min)[a]
					Type	wt %	Type	wt %	
KBO 01	100	0	0	0	—	0	—	0	15
KBO 02	92.5	0	0	0	Nanofil 919	7.5	—	0	8
KBO 03	0	100	0	0	—	0	—	0	0.3
KBO 04	0	85	0	7.5	Nanofil 15	7.5	—	0	0.8
KBO 05	19	76	5	0	—	0	—	0	9
KBO 06	12	75.5	5	0	Nanofil 919	7.5	—	0	8
KBO 07	16.5	67	4	0	Talc A7	12.5	—	0	4
KBO 08	12.5	65	4	5.5	Nanofil 919	7.2	Nanofil 15	5.8	5
KBO 09	12.5	68	0	6	Nanofil 919	7.5	Nanofil 15	6	7

[a] Melt flow rate (MFR) according to ISO 1133 at 230°C and 2.16 kg.

TABLE II
DSC and DMA Results

	DSC						DMA			
No.	T_m (PP) (°C)	H_m (PP) (J/g)	T_m (PA-6) (°C)	H_m (PA-6) (J/g)	T_o (PP) (°C)	T_o (PA-6) (°C)	T_g (PP) (°C)	T_{g1} (PA-6) (°C)	T_{g2} (PA-6) (°C)	T_g (SEBS) (°C)
KBO 01	—	—	213	89.6	—	190	—	−74	34	—
KBO 02	—	—	219	69.5	—	192	—	−74	32	—
KBO 03	164	107.1	—	—	119	—	6	—	—	—
KBO 04	164	99.0	—	—	121	—	2	—	—	—
KBO 05	164	81.0	219	11.9	118	183	8	−75	nd	−50
KBO 06	164	81.4	219	5.6	119	185	2	−75	nd	−50
KBO 07	164	69.9	219	10.7	121	190	6	−75	nd	−50
KBO 08	164	81.3	216	3.1	119	191	0	−75	nd	−50
KBO 09	164	80.4	218	2.7	120	190	−2	−75	nd	—

nd = not detectable.

polymer components; a standard PA-6, Durethan B30S (Bayer, Leverkusen, Germany), was used as the second blend component. Two different compatibilizers, which had turned out to be efficient in earlier studies on blends, were applied: Polybond 3200 (Crompton, Zwijndrecht, Belgium), a PP-*g*-MAH with a grafting degree of 0.5 wt % MAH, and Kraton FG1901X (Kraton Polymers, Houston, TX), a styrene elastomer (SEBS structure) grafted with MAH (styrene-ethylene-butadiene-styrene copolymer (SEBS)-*g*-MAH).

Both nanofillers used—Nanofil 15, which is suitable for polyolefins (with distearyl dimethyl ammonium chloride modification), and Nanofil 919, which is recommended for polycondensates (with stearyl dimethyl benzyl ammonium chloride modification)—were supplied by Süd-Chemie AG (Moosburg, Germany). A nontreated talc, Luzenac A7 (top cut = 7 μm, average particle size = 1.8 μm; Luzenac, Toulouse, France), was used as a reference mineral filler.

The preparation of the blends was carried out in multiple extrusion steps in any case. First, nanocomposites based on PP or PA-6 were prepared by the melt compounding of the polymer with nanoclay, followed by the blending of the nanocomposites with either a pure polymer or a nanocomposite into nanoblends with montmorillonite in either one or both of the polymer phases. The compounding was performed on a corotating twin-screw extruder (ZE25, Berstorff, Hannover, Germany) with a length of 36 D at a screw speed of 300 min^{-1}, a throughput of 10 kg/h, and temperature settings between 200 and 220°C for PP and between 250 and 230°C for PA-6 and blend nanocomposites, and the composites were finally pelletized from strands solidified in a water bath.

For the PA-6 nanocomposites, only one compounding step was required, for which both the polymer granules and the nanofiller were fed into the main hopper, the extrusion being run with vacuum degassing at 28 D. The PP nanocomposites were produced

TABLE III
Mechanical Properties ISO Tests were Done on Injection-Molded Specimens; DMA Tests were Done on Compression-Molded Plaques

		Charpy ISO 179 1eA		G' (DMA)	
No.	Flexural test modulus (MPa)	23°C (kJ/m^2)	−20°C (kJ/m^2)	23°C (MPa)	80°C (MPa)
KBO 01	2710	3.6	3.0	789	163
KBO 02	3890	2.7	2.5	1153	336
KBO 03	1630	19.1	2.8	695	152
KBO 04	2150	16.5	2.2	912	209
KBO 05	1550	23.7	6.7	576	117
KBO 06	1380	7.4	3.0	683	157
KBO 07	2190	19.6	7.2	883	192
KBO 08	1650	6.3	3.4	814	187
KBO 09	2080	4.9	2.0	950	272

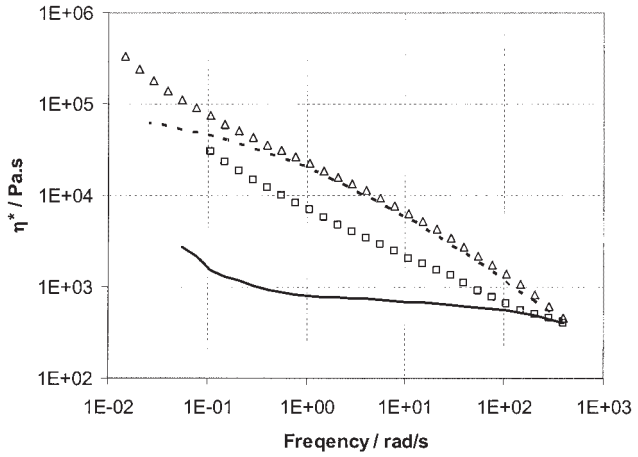

Figure 1 Complex viscosities of pure matrix polymers (—) PA-6 (KBO 01) and (- - -) PP (KBO 03) and single-polymer nanocomposites of (□) PA-6 (KBO 02) and (△) PP (KBO 04), as calculated by the Cox–Merz rule from $G'(\omega)$ and $G''(\omega)$ at 230°C (storage and loss modulus).

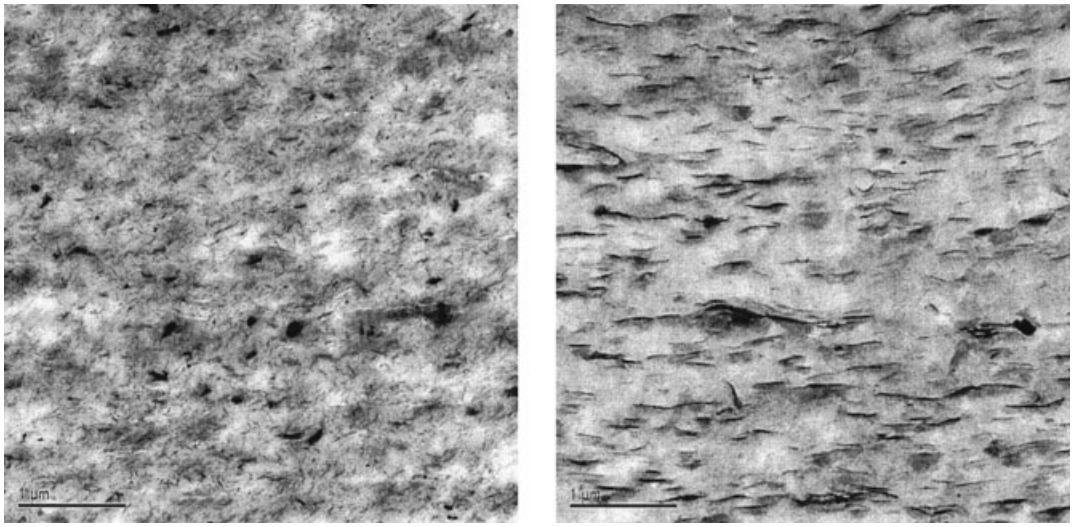

Figure 2 Nanofiller dispersion images (TEM micrographs after RuO_4 staining) of single-polymer nanocomposites of PA-6 (KBO 02; left) and PP (KBO 04; right).

in two steps: first, the compatibilizer and the nanofiller (batch preparation) were combined, and then this compound was diluted with the base PP polymer to the target clay content. Table I gives the compositions of all the investigated systems.

Morphological and rheological characterization

The blend structure—the phase distribution and nanofiller dispersion—was mainly evaluated with electron microscopy techniques. Two different approaches were tried successfully: scanning electron microscopy (SEM) on cold-cut surfaces etched with formic acid to remove the PA-6 phase and transmission electron microscopy (TEM) on ultramicrotomed specimens after contrasting with RuO_4. However, TEM investigations on cryofractured surfaces gave a rather unclear picture. SEM was performed on a Leo VP 435 (Zeiss, Oberkochen, Germany), and TEM was performed on a Tecnai G^2 12 (FEI Co., Hillsboro, OR) equipped with a charge-coupled device camera (Gatan Bioscan, Gatan, Pleasanton, CA) at 100 kV.

For checking the actual degree of exfoliation of the nanofillers, small-angle X-ray diffraction of the pure nanoclays as well as some selected compositions was performed with a Kratky camera (O. Paar, Graz, Austria).

Rheological investigations have been found to be useful for understanding both morphology development in polymer blends[5,30] and the quality of the filler dispersion.[31] Dynamic mechanical measurements in plate–plate geometry at 230°C were used for characterizing the nanoblends. The measurements were performed on an ARES instrument (Rheometrics, now TA Instruments, Crawley, UK), starting with compression-molded plaques and scanning from high to low frequencies.

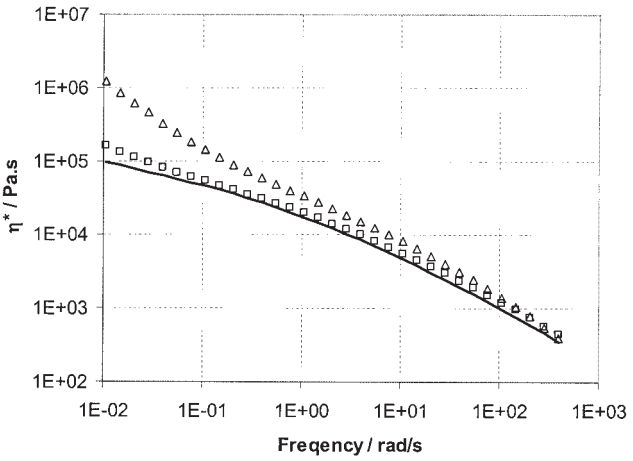

Figure 3 Complex viscosities of PP/PA-6 blends (—) without nanofillers (KBO 05), (□) with 12.5 wt % talc (KBO 07), and (△) with 12.7 wt % nanofiller combination (KBO 08), as calculated by the Cox–Merz rule from $G'(\omega)$ and $G''(\omega)$ at 230°C.

Thermal and thermomechanical characterization

The melting and crystallization behavior of the nanocomposite compositions was investigated with differential scanning calorimetry (DSC) at heating and cooling rates of 20 K/min with a Q1000 (TA Instruments). Dynamic mechanical analysis (DMA) at a frequency of 1 rad/s and a heating rate of 2 K/min was carried out to determine mobility transitions, with the same sample preparation and instrument used for the rheological measurements. Table II summarizes the glass-tran-

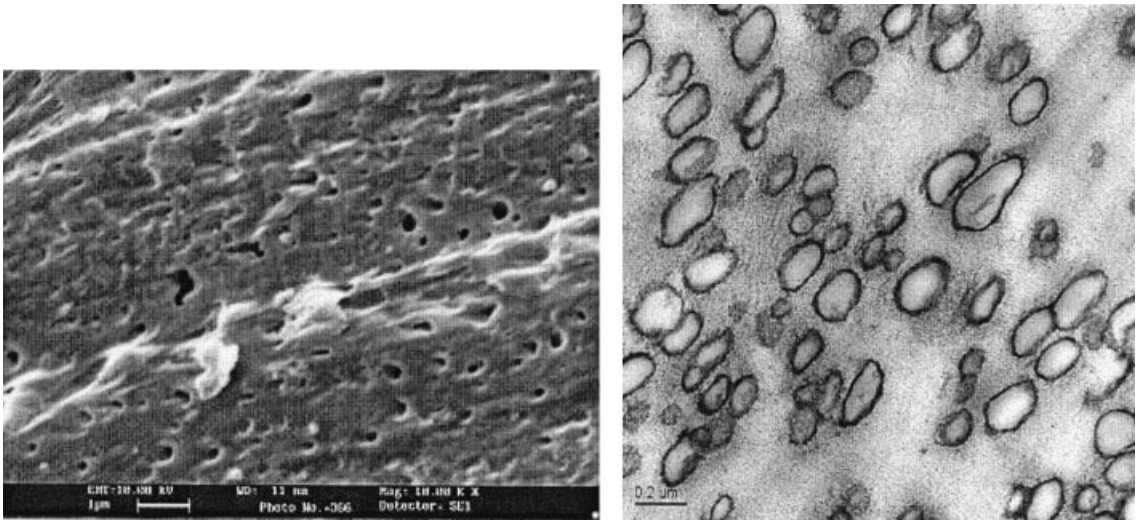

Figure 4 Morphology of a PP/PA-6 blend (KBO 05): a comparison of an etched SEM image after cutting (left) and a RuO_4-stained TEM micrograph (right) for phase-structure analysis.

sition temperature (T_g), peak melting temperature (T_m), and peak crystallization temperature (T_c).

The mechanical performance of all compounded materials was evaluated from injection-molded specimens (injection molding machine, Demag, Schwaig, Germany) in the dry (as-molded) state. The flexural modulus (ISO 178) and Charpy notched impact strength (ISO 179 1eA at +23 and −20°C) for specimens of $80 \times 10 \times 4$ mm^3 were determined; the results are summarized in Table III.

RESULTS AND DISCUSSION

Morphology and rheology

As already known from the field of polymer blends in general, the rheology and morphology of a multiphase material are closely linked. The ratio between the complex viscosities of the matrix and disperse phase of a two-phase system defines the resulting phase structure, whereas this morphology again affects the flowability of the final material. In the case of the materials studied here, which more or less have a PP/PA-6 composition of 80/20 (w/w), the particle size of the disperse (PA-6) phase will be defined by the aforementioned ratio.

The two polymer components were selected so that the higher viscosity of the continuous (PP) phase over a wide shear rate range would ensure good dispersion of the PA-6 phase (see Fig. 1). The addition of 7.5 wt % organoclay has, however, quite different effects on the two polymers: Although the viscosity increase is limited to the very low shear rate range (essentially

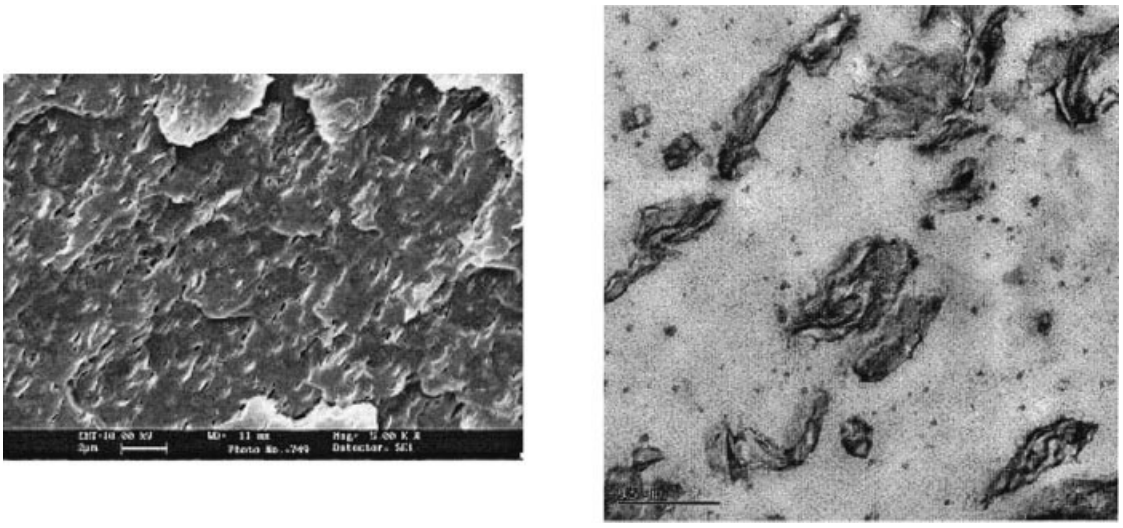

Figure 5 Morphology of a PP/PA-6 nanocomposite (KBO 08): a comparison of an etched SEM micrograph after cryofracturing (left) and a TEM micrograph (right) for phase-structure analysis.

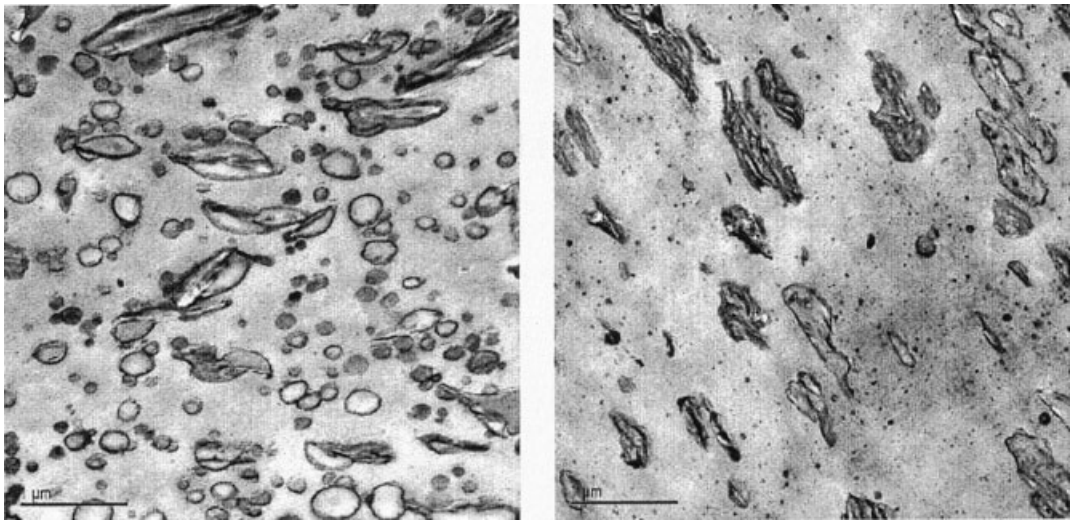

Figure 6 Filler dispersion images (TEM micrographs after RuO_4 staining) of PP/PA-6 blends with talc (KBO 07, left) and Nanofil 919 (KBO 06, right).

resulting from a low frequency plateau of storage modulus (G')) for PP, the flow curve is altered completely for PA-6. As Figure 2 shows, this results from a rather obvious difference in the degree of dispersion (even if the addition of the low-viscosity compatibilizer, PP-*g*-MAH, will also affect the viscosity in the case of the PP nanocomposite). The number of nonexfoliated, thicker stacks and nonintercalated structures is significantly higher in the case of PP; this fact is also reflected in the small-angle X-ray scattering (SAXS) investigation discussed later.

Although the rheology of the PP/PA-6 blends is again rather weakly affected by the filler addition (see Fig. 3), their morphology reflects the difference in the phase viscosity relation from Figure 1. In the case of the pure blend (see Fig. 4), a rather homogeneous distribution of PA-6 particles with a diameter of ~0.2 μm can be seen, practically all of these revealing an interfacial structure typical of the use of SEBS-*g*-MAH as a compatibilizer, in which the polystyrene domains are clearly visible at higher magnifications (see also the TEM images in ref. 20). The so-formed soft coupling of the two polymer phases allows rather high toughness levels, which are retained at subzero temperatures because of the low T_g of SEBS.

When nanofillers are added to both polymer components before blending, two things can be observed:

- The phase structure becomes much coarser (see Fig. 5), and most of the nanofiller particles end up in the PA-6 phase. Figures 4 and 5 also show that much more detailed structural information is obtainable with the stained TEM micrographs in comparison with the SEM images.
- The greater affinity to the more polar polycondensate phase is not limited to the nanofillers (for which the differences in the surface treatment between the two applied grades do not affect the distribution). As Figure 6 illustrates, the talc particles are more likely to be covered by a PA-6 layer or particle than to be dispersed in the PP phase. The aforementioned phase-coarsening effect is especially dramatic for the combination of pure PP with the PA-6 nanocomposite in KBO 06.

The dispersion quality and agglomeration effects are also reflected in the SAXS diagrams. Although the sole use of this method to evaluate the degree of exfoliation of a nanocomposite is not recommended and gives only a semiquantitative picture because of dilution effects and the failure to reflect major agglomerations, it is a very useful tool for checking actual intercalation and exfoliation phenomena. The strong difference between the polyolefin with the nanofiller and the polycondensate with the nanofiller, already outlined before, can also be seen in Figures 7 and 8. Although in the case of PP, even with the addition of compatibilizers, only dilution effects can be observed (KBO 04), the PA-6 nanocomposite (KBO 02) shows both intercalation and at least partial exfoliation. In the blend system, this effect appears partially reversed, probably because of the very high filler concentration inside the PA-6 particles, as obtained from the morphology images in Figures 4–6.

Crystallization behavior

Changes in the crystallization behavior can strongly affect the mechanical performance of any polymer/mineral hybrid material. This is especially true for processing-related effects, in which flow-induced crystallization and the development of superstructures (skin layers, etc.) play a major role. Such phenomena

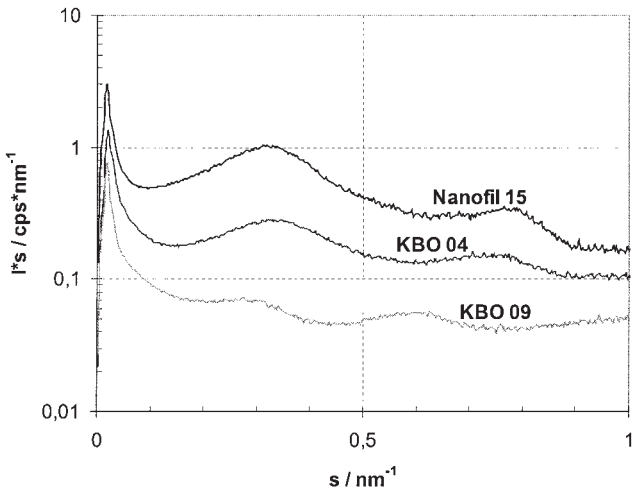

Figure 7 SAXS diagram for Nanofil 15, the respective PP nanocomposite (KBO 04), and the nanoblend containing both nanoclay types (KBO 09). I*s = intensity.

have, among others, been investigated for PP/talc compounds[32,33] and also for PA-6 nanocomposites.[15] In both cases, the combined effects go beyond the simple nucleation observed in the quiescent state.

Two interactions have to be considered for the crystallization in PP/PA-6 nanocomposites: (1) between PP and PA-6 and (2) between the polymer and mineral. In the first case, two effects have been reported in the blend literature, namely, a nucleation of the PP phase, especially in the case of finely dispersed PA-6 particles[19,20] and a suppression of the PA-6 crystallization and a shift to lower T_c's (together with PP at ~115°C[17,18] or in a secondary peak ca. 86°C[20]). As can be seen in Table II, only the first effect could be found in this study. If compound KBO 05 is considered mainly (no filler), both the melting and crystallization enthalpies of the PA-6 phase are lower than expected because of the partial coupling to the compatibilizer and/or the crystallization under confined conditions inside the silicate layers and between the particles.

For the second case, most authors report a nucleation of PA-6 by adding nanofillers,[14,16] sometimes together with an increased presence of the γ modification of the crystalline phase. In our investigation, this could be found only for the pure PA-6 nanocomposite; in the blends containing nanofiller, the suppression of crystallization is actually stronger than in the pure blend, again in line with earlier results.[14] The weak nucleation of PP by the organoclay, also claimed in the literature,[34] results from a combination effect with the compatibilizer, as already the presence of small amounts of PP-*g*-MAH increases T_c of PP. No crystallinity reduction was observed for this phase.

Generally, a plot of the melting enthalpy (H_m; PA-6) over the weight fraction of PA-6 shows all values to be lower than expected from a mixing rule, whereas in an analogous plot for PP, most of the enthalpy values are higher than expected.

Mechanical properties

An overview of the thermomechanical behavior of the investigated systems can already be gained from DMA measurements, which have been demonstrated to be

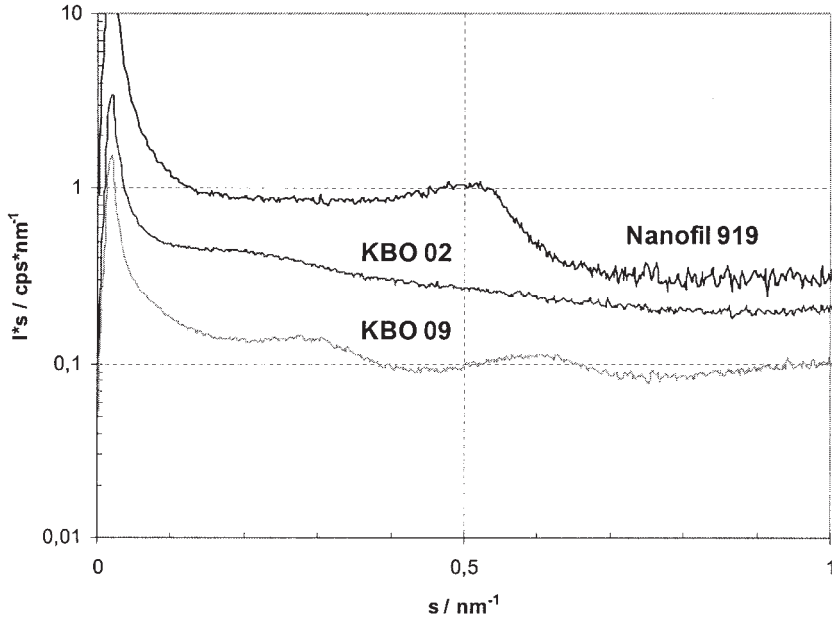

Figure 8 SAXS diagram for Nanofil 919, the respective PA-6 nanocomposite (KBO 02), and the nanoblend containing both nanoclay types (KBO 09). I*s = intensity.

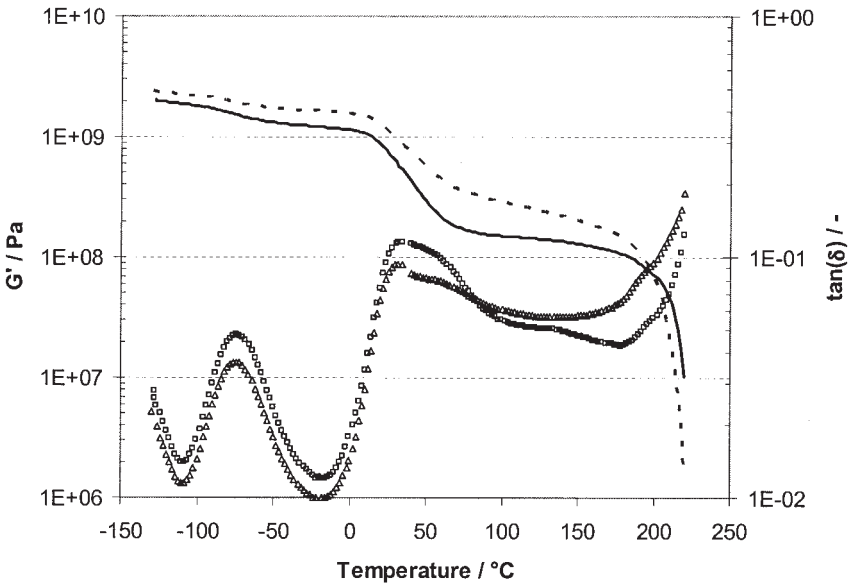

Figure 9 DMA scan of the thermomechanical behavior of PA-6 [KBO 01; (—) G' and (□) tan δ] and the PA-6 nanocomposite [KBO 02; (- - -) G' and (△) tan δ].

very useful even for the prediction of standard mechanics with comparatively small sample quantities.[35,36] In Table III, the storage modulus values for both +23 and +80°C are given to also get an impression of the high-temperature performance of the materials (for which the normal heat deflection temperature measurements, e.g., HDT ISO 75 B, only give a single-point value). Differences in the softening behavior between the neat polymers (or blends) and the respective nanocomposites are obvious in both Figures 9 and 10. In the correlation between G' (+23°C) and the flexural modulus, however, the variation of PA-6 and filler content causes a massive scatter similar to the one reported previously for PP nanocomposites.[35]

An interesting effect not found in the respective blend literature is the disappearance of the second glass transition of the PA-6 phase at ~34°C in the blends and nanoblends (see Table II). As this is supposed to be a crystalline mobility transition such as $T_{\alpha,c}$ in PP (50–90°C), the effect can well be linked to the aforementioned crystallization suppression.

The general overview of standard mechanics in Figure 11 shows the problems of property optimization in the investigated systems. The addition of nanoclays just like

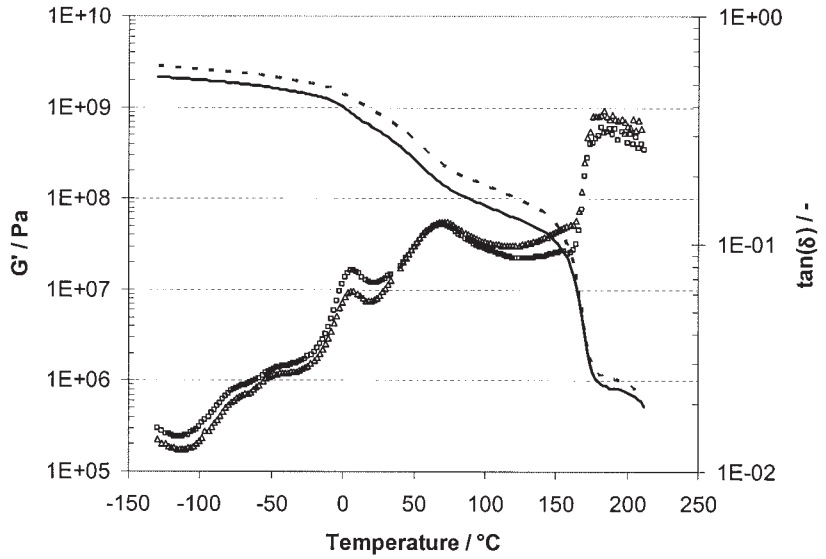

Figure 10 DMA scan of the thermomechanical behavior of the PP/PA-6 blend [KBO 05; (—) G' and (□) tan δ] and the PP/PA-6 nanocomposite [KBO 08; (- - -) G' and (△) tan δ].

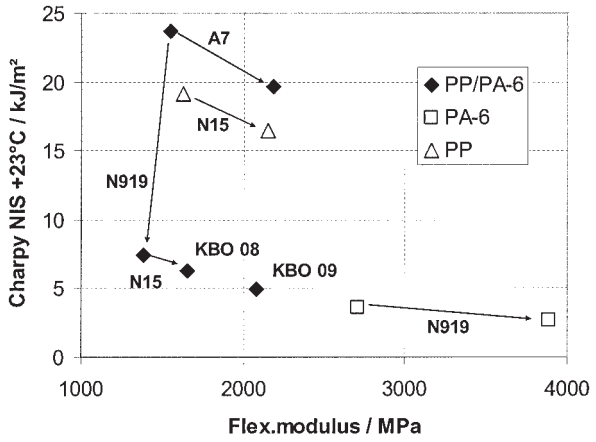

Figure 11 Mechanical profile of all investigated compounds (the symbols indicate respective base polymers, and the arrows indicate single filler effects; NIS = notched impact strength, N15 = Nanofil 15, N919 = Nanofil 919, A7 = Luzenac A7).

the addition of a comparable amount of a standard mineral filler leads to a toughness reduction in all cases, whereas the modulus increase is strongest in the pure PA-6 matrix.

CONCLUSIONS

PP/polyamide (PA) blends and their nanocomposites with layered silicates or talc were prepared to explore the potential of such nanocomposite blends as new materials with high mechanical performance. A two-step melt-compounding process was applied: first, the nanocomposites, consisting of the clay and polymer, were processed, and then they were mixed into the final nanocomposite blend. The melt viscosities of the polymers and compatibilizers were adjusted to obtain optimal mixing and phase adhesion. It was shown by electron microscopy methods that in all cases the inorganic filler was enriched in the PA phase, and this resulted in a phase coarsening in comparison with the nonfilled PP/PA blend. In none of the compositions could the earlier described labyrinth structure,[29] in which the clay is found mainly at the interface between the two polymers, be found. As a reason, the higher affinity of the polar layered silicates (even after organophilic modification) to the more polar PA phase than to the apolar PP phase could be discussed. As a result of this preferential reinforcement of the PA phase, the mechanical properties of these nanoblends were only slightly better than those of the pure polymers with respect to the modulus, whereas the impact property level was below that of the pure polymers, reflecting the heterogeneity of the nanoblend.

The authors thank Bernhard Knogler (Borealis) for carrying out the rheology and dynamic mechanical analysis investigations, Liane Häußler (Institut für Polymerforschung) for the differential scanning calorimetry measurements, Dieter Jehnichen and Jan Müller (Institut für Polymerforschung) for the small-angle X-ray scattering investigations, Petra Pötschke (Institut für Polymerforschung) for the scanning electron microscopy imaging, and finally Kshama Motha and Tung Pham (Borealis) for helpful discussions.

References

1. Mitsuishi, K.; Kodama, S.; Kawasaki, H. J Macromol Sci Phys 1987, 26, 479.
2. Xavier, S. F.; Schultz, J. M.; Friedrich, K. J Mater Sci 1990, 25, 2411.
3. Svehlova, V.; Poloucek, E. Angew Makromol Chem 1994, 214, 91.
4. Bernreitner, K.; Hammerschmid, K. In Polypropylene—An A to Z Reference; Karger-Kocsis, J., Ed.; Kluwer Academic: Dordrecht, 1999; p 148.
5. Scholz, P.; Froehlich, D.; Muller, R. J Rheol 1989, 33, 481.
6. Rösch, J.; Mülhaupt, R. J Appl Polym Sci 1995, 56, 1607.
7. Ohlsson, B.; Hassander, H.; Törnell, B. Polymer 1998, 39, 4715.
8. Shi, D.; Ke, J.; Yang, J.; Gao, Y.; Wu, J.; Yin, J. Macromolecules 2002, 35, 8005.
9. Sacchi, A.; Di Landro, L.; Pegorato, M.; Severini, F. Eur Polym J 2004, 40, 1705.
10. Harmia, T.; Friedrich, K. Compos Sci Technol 1995, 53, 423.
11. Wong, S.-C.; Mai, Y.-W. Polym Eng Sci 1999, 39, 356.
12. Forbes, T. D.; Yoon, P. J.; Keskkula, H.; Paul, D. R. Polymer 2001, 42, 9929.
13. Dennis, H. R.; Hunter, D. L.; Chang, D.; Kim, S.; White, J. L.; Cho, J. W.; Paul, D. R. Polymer 2001, 42, 9513.
14. Liu, X.; Wu, Q. Eur Polym J 2002, 38, 1383.
15. Yalcin, B.; Valladares, D.; Cakmak, M. Polymer 2003, 44, 6913.
16. Lincoln, D. M.; Vaia, R. A.; Krishnamoorti, R. Macromolecules 2004, 37, 4554.
17. Psarski, M.; Pracella, M.; Galeski, A. Polymer 2000, 41, 4293.
18. Laurens, C.; Ober, R.; Creton, C.; Léger, L. Macromolecules 2001, 34, 2932.
19. Pompe, G.; Pötschke, P.; Pionteck, J. J Appl Polym Sci 2002, 86, 3445.
20. Wilkinson, A. N.; Clemens, M. L.; Harding, V. M. Polymer 2004, 45, 5239.
21. Chundury, D. (to Ferro Corp.). U.S. Pat. 5,278,231 (1990).
22. Koehler, K.-H.; Reinking, K. (to Bayer AG). Eur. Pat. EP 244601 A2 (1987).
23. Ray, S. S.; Okamoto, M. Prog Polym Sci 2003, 28, 1539.
24. Korbee, R. A.; Van Geenen, A. A. (to DSM NV). Pat. WO 9929767 A1 (1997).
25. Maxfield, M.; Shacklette, L. W. (to Allied Signal, Inc.). Eur. Pat. EP 598836 B1 (1991).
26. Liu, X.; Wu, Q.; Berglund, L. A.; Fan, J.; Qi, Z. Polymer 2001, 42, 8235.
27. Tjong, S. C.; Meng, Y. Z.; Xu, Y. J Appl Polym Sci 2002, 86, 2330.
28. Chow, W. S.; Mohd Ishak, Z. A.; Karger-Kocsis, J.; Apostolov, A. A.; Ishiaku, U. S. Polymer 2003, 44, 7427.
29. Tang, Y.; Hu, Y.; Zhang, R.; Gui, Z.; Wang, Z.; Chen, Z.; Fan, W. Polymer 2004, 45, 5317.
30. Gahleitner, M. Prog Polym Sci 2001, 26, 895.
31. Gahleitner, M.; Bernreitner, K.; Neißl, W. J Appl Polym Sci 1994, 53, 238.
32. Fujiyama, M.; Wakino, T. J Appl Polym Sci 1991, 42, 2749.
33. Fujiyama, M. Int Polym Proc 1992, 7, 358.
34. Krishnamoorti, R.; Yurkeli, K. Curr Opin Colloid Interface Sci 2001, 6, 464.
35. Gahleitner, M.; Grein, C.; Hauer, A.; Motha, K. Proceedings of the PPS Europe–Africa Conference 2003, Athens, Greece [CD-ROM]; Lecture 11-A1-O; Polymer Processing Society: Akron, OH.
36. Grein, C.; Bernreitner, K.; Gahleitner, M. J Appl Polym Sci 2004, 93, 1854.